ORIGINAL ARTICLE

Primary Cutaneous Aspergillosis in a Patient with CARD9 Deficiency and *Aspergillus* Susceptibility of *Card9* Knockout Mice

Yi Zhang [1,2,3,4] · Chen Huang [1,2,3,4] · Yinggai Song [1,2,3,4] · Yubo Ma [1,2,3,4] · Zhe Wan [1,2,3,4] · Xuejun Zhu [1,2,3,4] · Xiaowen Wang [1,2,3,4] · Ruoyu Li [1,2,3,4]

Abstract

Purpose We describe a case of primary cutaneous aspergillosis caused by *Aspergillus fumigatus*, and elucidate the underlying genetic and immunological mechanisms.

Materials and Methods Routine clinical and laboratory investigations were performed. Whole-exome sequencing of the patient's DNA suggested the presence of a *CARD9* mutation, which was confirmed by Sanger sequencing. Innate and adaptive immunological responses of patient-derived CARD9-deficient cells were evaluated with ELISA and flow cytometry. Cutaneous and pulmonary aspergillosis models were established in *Card9* knockout (KO) mice, which were compared with wild-type and immunosuppressed mice, to explore the pathogenesis and *Aspergillus* susceptibility.

Results A 45-year-old man presented with a 37-year history of skin lesions on his face. A diagnosis of primary cutaneous aspergillosis was made through histopathology, immunohistochemistry, and tissue culture. Sanger sequencing of *CARD9* showed a homozygous frame-shift mutation (c.819_820insG, p.D274fsX60), which led to the lack of CARD9 expression. Peripheral blood mononuclear cells from the patient showed selective impairment of proinflammatory cytokines, and Th1-, Th17-, and Th22-associated responses upon fungus-specific stimulation. The cutaneous aspergillosis model established in *Card9* KO mice presented with persistent infection, with fungal germs and short hyphae in tissue, consistent with the patient's lesions. Skin lesions in immunosuppressed mice were more severe, and led to death. Unlike our patient, *Card9* KO mice were relatively susceptible to pulmonary aspergillosis, with reasons to be investigated.

Conclusions This is, to our knowledge, the first report that links cutaneous aspergillosis to *CARD9* mutation. This work enriches both the phenotypic spectrum of CARD9 deficiencies and the genetic background of cutaneous aspergillosis.

Keywords Primary cutaneous aspergillosis · *Aspergillus fumigatus* · CARD9 · knockout mice

Xiaowen Wang and Ruoyu Li contributed equally to this work.

✉ Xiaowen Wang
xiaowenpku@126.com

✉ Ruoyu Li
mycolab@126.com

1   Department of Dermatology and Venerology, Peking University First Hospital, No. 8 Xishiku Street, Xicheng District, Beijing 100034, China

2   Research Center for Medical Mycology, Peking University, Beijing, China

3   Beijing Key Laboratory of Molecular Diagnosis on Dermatoses, Beijing, China

4   National Clinical Research Center for Skin and Immune Diseases, Beijing, China

Introduction

Primary cutaneous aspergillosis (PCA) is an uncommon infection caused by *Aspergillus* spp., in which an infected skin lesion is the initial source of disease [1]. This is in contrast to secondary cutaneous aspergillosis, a more common form, which involves the hematogenous spread of *Aspergillus* infection from a distal site (e.g., the lungs) to the skin [1]. Clinically, PCA may present with various manifestations, such as paronychia, cellulitis, ulceration, pustules, papules, plaques, and blisters, as well as crusted lesions, nodules, or abscesses [2]. PCA is generally reported in immunosuppressed hosts, but rarely in immunocompetent individuals [3].

During pattern recognition of fungi, a key adaptor called caspase-associated recruitment domain-9 (CARD9) transduces signals downstream of different C-type lectin receptors

(CLRs, e.g., Dectin-1, Dectin-2, Dectin-3, and Mincle), through the SYK activation of ITAM, leading to activation of the NF-κB and MAPK pathways and the production of proinflammatory cytokines [4]. In the past decade, an increasing number of patients with inherited *CARD9* mutations have been reported to be predisposed to various fungal infections, including subcutaneous and invasive candidiasis, dermatophytosis, and dematiaceous fungal infections [5]. Herein, we report a case of PCA caused by *Aspergillus fumigatus* in a patient harboring a *CARD9* mutation. This is, to our knowledge, the first report that links cutaneous aspergillosis to *CARD9* mutation. A murine cutaneous aspergillosis model was established to explore the pathogenesis of PCA and susceptibility of *Card9* KO mice to *Aspergillus*.

Materials and Methods

Patient

A 45-year-old man, born to nonconsanguineous parents from Hebei Province, presented with erythematous plaques on his face with a history of 37 years. The patient denied any immunosuppressive conditions and recallable trauma. Histological and immunohistochemical examinations, together with mycological examinations, including direct microscopic examination, fungal culture, and fungal gene sequencing, were carried out. Fungal genomic DNA was extracted from cultures grown on potato dextrose agar (PDA; BD Biosciences, San Jose, CA, USA) and sequenced as previously described [6]. The internal transcribed spacer (ITS) region, β-tublin, actin, and calmodulin genes were sequenced and aligned using CBS-KNAW (Westerdijk Fungal Biodiversity Institute, Ultretch, The Netherlands) for identification of the fungus. The routine blood examinations, serologic testing for galactomannan (GM test) and 1,3-beta-D-glucan (G test), and pulmonary CT scan were also conducted.

Patient DNA Extraction, Whole-Exome Sequencing, and Sanger Sequencing

Genomic DNA was extracted from the peripheral blood of the patient and his son. Exome capture was carried out with Agilent Bioanalyzer 2100 (Agilent) to examine the quality of the DNA sample in the captured library, and then sequenced using the NEXTSEQ500 System (Illumina) according to the concentration and depth requirement of the DNA sample in the captured library, following the manufacturer's protocols. Upon comparison of these variants with the genes previously reported to be implicated in fungal infection, we could find only one gene (*CARD9*). Sanger sequencing was subsequently performed to validate the mutation in *CARD9*.

Isolation of Human Peripheral Blood Mononuclear Cells and Immunoblot Analyses for CARD9

Human peripheral blood mononuclear cells (PBMCs) were isolated from the whole blood by density-gradient centrifugation using the Ficoll-Paque Plus (GE Healthcare, Chicago, IL, USA). Protein extracts were prepared using the whole protein extraction kit (KeyGEN BioTECH) according to the protocol provided by the manufacturer. The proteins were separated by electrophoresis on a 10% SDS-polyacrylamide gel and transferred onto nitrocellulose membranes. The blots were probed with rabbit anti-human CARD9 (Cell Signaling Technology and Abcam) or rabbit anti-GAPDH (Proteintech) primary antibodies, and later incubated with HRP-conjugated anti-rabbit IgG. The anti-human CARD9 antibody from Cell Signaling Technology was produced by immunizing animals with a synthetic peptide corresponding to residues near the carboxy terminus of human CARD9 protein. The immunogen from Abcam was synthetic peptide corresponding to residues in Human CARD9 467 to 480 ALHQ EQVLRNPHDA. The immunoreactive bands were visualized by chemiluminescence using an ECL substrate (Thermo Scientific Pierce, Waltham, MA, USA) and analyzed with the Image Quant LAS 500 system (GE Healthcare).

PBMC Stimulation Assay

A. fumigatus isolates were cultured on potato dextrose agar (PDA; BD Biosciences, San Jose, CA, USA) for 4 days at 37 °C to harvest conidia. Heat-killed (HK) conidia required for stimulation were prepared by heating at 90 °C in a water bath for 30 min. For analysis of cytokines involved in innate immunity by ELISA, PBMCs from the patient and four healthy controls were cultured to a final concentration of 2.5×10^6/mL in a total volume of 200 μL and stimulated for 24 h with pattern recognition receptor agonists, including lipopolysaccharide (LPS; 100 ng/mL), curdlan (100 μg/mL), trehalose-6,6-dibehenate (TDB; 100 μg/mL), mannan (100 μg/mL), and *A. fumigatus* (HK or viable resting conidia, 10^7 particles/mL), at 37 °C in an atmosphere of 5% CO_2. To assess the adaptive immune response, PBMCs were stimulated with curdlan (100 μg/mL), TDB (100 μg/mL), mannan (100 μg/mL), and *A. fumigatus* (HK resting conidia, 10^7 particles/mL), for 6 days, and cells or culture supernatants were collected for flow cytometry and ELISA assays.

Measurement of Cytokines and Intracellular Staining of Cytokines in CD4+ T Cells

The levels of cytokines were measured in the supernatants harvested, 24 h or 6 days after stimulation, using ELISA kits (R&D Systems, Minneapolis, MN, USA), according to the manufacturer's instructions. Intracellular staining for IFN-γ,

IL-17A, and IL-22 was performed on PBMCs stimulated for 5 h with Cell Stimulation Cocktail (eBioscience, San Diego, CA, USA) after incubating them for 6 days with different pattern recognition receptor agonists and HK *A. fumigatus* conidia. FITC-labeled anti-CD4 was added for the final 30 min of culture before the fixing and permeabilization steps. The cells were then washed with PBS and stained with PerCP-Cy5.5-conjugated anti-human IFN-γ, Alexa®Fluor647-conjugated anti-human IL-17A, and PE-conjugated anti-human IL-22 antibodies. Data were acquired on a BD FACS Calibur system and analyzed with the FlowJo7.6 software.

Assay of NF-κB p65 Phosphorylation by Dynamic Phospho-flow Cytometry

Phospho-flow analysis of NF-κB p65 phosphorylation at serine 536 was conducted according to the manufacturer's instructions. Briefly, PBMCs (2.5×10^6/mL) were stimulated with HK *A. fumigatus* conidia (1×10^7/mL) for 30 min and then fixed using prewarmed Cytofix buffer (BD Biosciences). Thereafter, the cells were stained with APC anti-human CD14 antibody, permeabilized with chilled Perm buffer III (BD Biosciences), and incubated with Alexa Fluor 488–conjugated Phospho-NF-κB p65 (Ser536) rabbit monoclonal antibody (BD Biosciences). An Alexa Fluor 488–conjugated rabbit IgG isotype was used as a control. Data were acquired on a BD Biosciences FACS Calibur system and analyzed with the FlowJo 7.6 software.

Mouse Model of Aspergillosis

To investigate the mechanism of PCA with CARD9 deficiency, we utilized WT (C57BL/6, 6–8-week-old), *Card9* KO (C57BL/6, 6–8-week-old), and immunosuppressed mice (BALB/c, 6–8-week-old) to mimic primary cutaneous and pulmonary aspergillosis. WT, *Card9* KO, and immunosuppressed mice (Vital River Laboratories, Beijing, China) were maintained in specific pathogen-free facilities at the Institute of Clinical Pharmacology of Peking University. BALB/c mice were immunosuppressed by injecting a combination of cyclophosphamide and cortisone acetate. Four days and 1 day prior to the inoculation, initial doses of 150 mg/kg cyclophosphamide were given to the mice intraperitoneally. Three days prior to the inoculation, doses of 200 mg/kg cortisone acetate were given to the mice intraperitoneally. In addition, these mice received water containing 200 μg/mL doxycycline hyclate to prevent bacterial infections caused as a consequence of immunosuppression induced for the duration of the study. To extend the duration of neutropenia, a new cycle of immunosuppression was initiated on day 2 post-infection with the same dose of cyclophosphamide (150 mg/kg).

For establishing the cutaneous aspergillosis model, 100 μL viable *A. fumigatus* conidia (2.5×10^9/mL) were subcutaneously injected in two hind footpads of mice. The natural course of infection was monitored weekly for 4 weeks after the injection. Skin biopsy specimens were obtained, and slides were prepared and stained with periodic acid–Schiff (PAS) for histological analysis. Fungal burdens of infected footpads were determined at day 3 post-infection by plating serially diluted footpad homogenates on potato dextrose agar (PDA; BD Biosciences, San Jose, CA, USA). At day 3, 5, 7, 14, 21, and 28 post-infection, mice were euthanized and their lungs, kidneys, livers, spleens, and brains were obtained for fungal burden detection and histopathology.

To compare local immune responses in these three groups, skin tissue obtained from the infected footpads on day 3 was lysed in chilled saline using tissue grinders. The supernatant collected after centrifugation of the skin homogenate was evaluated for the levels of different cytokines using the Cytometric Bead Array (CBA) Mouse IL-6/TNF-α/IL-1β kit (BioLegend) and was analyzed by the LEGENDplex8.0 software (BioLegend). Total RNA was extracted from skin tissue on day 3 and 7 post-infection using Trizol reagent (Servicebio), following the manufacturer's instructions. cDNA synthesis was performed using the RevertAid First Strand cDNA Synthesis Kit (Thermo Scientific) according to the manufacturer's instructions. Quantitative real-time reverse transcriptase PCR was conducted using Power SYBR Green PCR Master Mix (Applied Biosystems, Thermo Fisher Scientific) on the 7500 Real-Time PCR system (Applied Biosystems, Thermo Fisher Scientific). The relative mRNA expression levels of proinflammatory cytokines (IL-1β, TNF-α, and IL-6) and neutrophils attracting chemokines (CXCL1, CXCL2, and CXCL5) were determined in day 3 samples, and those of adaptive cytokine (IFN-γ, IL-17A, and IL-22) were assessed in day 7 samples.

For establishing the pulmonary aspergillosis model, mice were lightly anesthetized and immobilized in an upright position. The optimum concentration of the conidial suspension (4×10^8/mL) was determined through a pre-experiment (2×10^8/mL or lower concentration was not sufficient to cause pulmonary infection). *A. fumigatus* conidial suspension (50 μL) was deposited in the nasal cavity of the mice while the diaphragm was lightly pressed; when it was released, the conidia were aspirated into the lungs. Mortality was monitored every day, and documented for 14 days after infection. At day 3, 5, 7, and 14 post-infection, mice were euthanized and their lungs, kidneys, livers, spleens, brains were obtained for fungal burden counting and histopathological analysis.

Local Neutrophil and T Lymphocyte Detection by FACS Analysis

To elucidate local immune cell infiltration, infected footpads were excised on day 3 and 7 post-infection, and were then washed in PBS and cut into pieces. After digesting in

preheated 0.25% Trypsin-EDTA (Gibco), the tissue precipitate was placed for 1 h in dissociation buffer containing collagenase IV (Solarbio), elastase (Macklin), CaCl$_2$ (Sigma-Aldrich), DNAase I (Sigma-Aldrich), and BSA (Miltenyi Biotec) at 37 °C twice. The digested tissue was filtered through a 40-μm cell strainer, and dead cells were removed by the Dead Cell Removal Kit (Miltenyi Biotec). Cells from the day 3 samples were incubated with FITC anti-mouse CD11b antibody (BioLegend) and APC anti-mouse Ly-6G antibody (BioLegend) to detect neutrophils. Cells from the day 7 samples were incubated with PE anti-mouse CD3 antibody (BioLegend) to detect T lymphocytes. Data were acquired on a BD FACS Calibur system and analyzed with the FlowJo7.6 software.

Statistical Analysis

The experimental data were represented using the GraphPad Prism 7.0 software (La Jolla, CA, USA) and analyzed using unpaired t test with the SPSS 22.0 software (Chicago, IL, USA). Statistical significance was defined as $P < 0.05$.

Results

Case Summary

A 45-year-old man, born to nonconsanguineous parents, presented to our dermatology clinic with a 37-year history of skin lesions on his face. He reported that he developed a soy-sized rash on his left eyelid without any trauma at the age of 8. The lesion slowly enlarged since then and progressed to involve his right eye during the past 3 years. The patient was otherwise healthy, and occasionally used topical antipruritic ointment on the lesion area to relieve itching during the past few years. Physical examination revealed erythematous plaques with clear border on his left face, eye circumference, bridge of nose, and right nasal side, with slight scale and crust. The left eyebrow was partially exfoliated, and the left eyelid was swollen and slightly desquamated without any atrophic change (Fig. 1a).

A biopsy specimen obtained from the left cheek revealed epidermal hyperplasia and inflammatory cells infiltrated in the dermis, including histocytes, multinuclear giant cells, eosinophils, plasma cells, and lymphocytes. It is noteworthy that a very limited number of neutrophils were scattered. PAS staining highlighted septate hyphae and germinated conidia in histocytes and multinuclear giant cells in the dermis (Fig. 1b). Direct microscopic examination of the lesion showed slender, septate, acute angle branched, hyaline hyphae (Fig. 1d). Cultures of the biopsied tissue specimens showed filamentous fungus. Colonies on PDA were dense and light green after 7 days at 28 °C (Fig. 1e). Further microscopic

examination of the cultured organisms revealed fruiting structures and globular conidiophores in lactophenol cotton blue stain (Fig. 1f). Only *A. fumigatus* was identified and confirmed by the sequencing of ITS, β-tublin, actin, and calmodulin genes. Immunohistochemistry using specific antibody against *Aspergillus* was positive (Fig. 1c; fungal elements seen in brown). Whole blood cell analysis including eosinophil counts showed no abnormality (Table S1), and serological testing was negative for GM and G tests. A CT scan excluded pulmonary aspergillosis. The patient responded well to oral itraconazole 400 mg/day. The lesion was observed to have improved significantly at follow-up after 2 months (Fig. S1). The patient stopped medication after treatment for 1 year with clinical cure, and is still under follow-up.

Homozygous *CARD9* Mutation and CARD9 Expression

To study the reason for the prolonged primary infection and to identify the genetic background in this otherwise healthy patient, whole-exome sequencing (WES) of the patient's genomic DNA was performed. Upon comparison of these variants with the genes previously reported to be implicated in fungal infection, we could find variations in only one gene (*CARD9*). Sanger sequencing of *CARD9* was subsequently performed to validate that the patient harbored a homozygous frame-shift mutation in exon 6 (c.819_820insG, p.D274fsX60), which led to premature termination codons (Fig. 2a). The parents of the patient found it inconvenient to visit our clinic. His son had a heterozygous mutation at the same locus (Fig. 2a). The expression of full-length wild-type CARD9 protein in PBMCs was absent in the patient through western blot analysis using both antibodies (Fig. 2b).

CARD9 Mutation Impaired the Fungus-Stimulated Production of Proinflammatory Cytokines and NF-κB Activation in the Patient

To evaluate the functional effects of CARD9 deficiency, we used PBMCs to examine the release of proinflammatory cytokines 24 h after stimulation with LPS (a Toll-like receptor 4 agonist), curdlan (a Dectin-1 agonist), TDB (a Mincle agonist), mannan (a Dectin-2 agonist), and fungal particles of *A. fumigatus* (HK or viable conidia). Compared with the PBMCs from healthy control participants, those from the patient showed markedly lower production of proinflammatory cytokines in response to curdlan, TDB, mannan, and *A. fumigatus*, whereas LPS stimulation remained unaffected or partially decreased, which indicates that *CARD9* mutation impaired the pattern recognition and production of cytokines involved in innate immune response in this patient (Fig. 3a–c). We next compared the NF-κB p65 phosphorylation in monocytes stimulated with the HK conidia of *A. fumigatus*. Monocytes from the patient showed diminished NF-κB p65
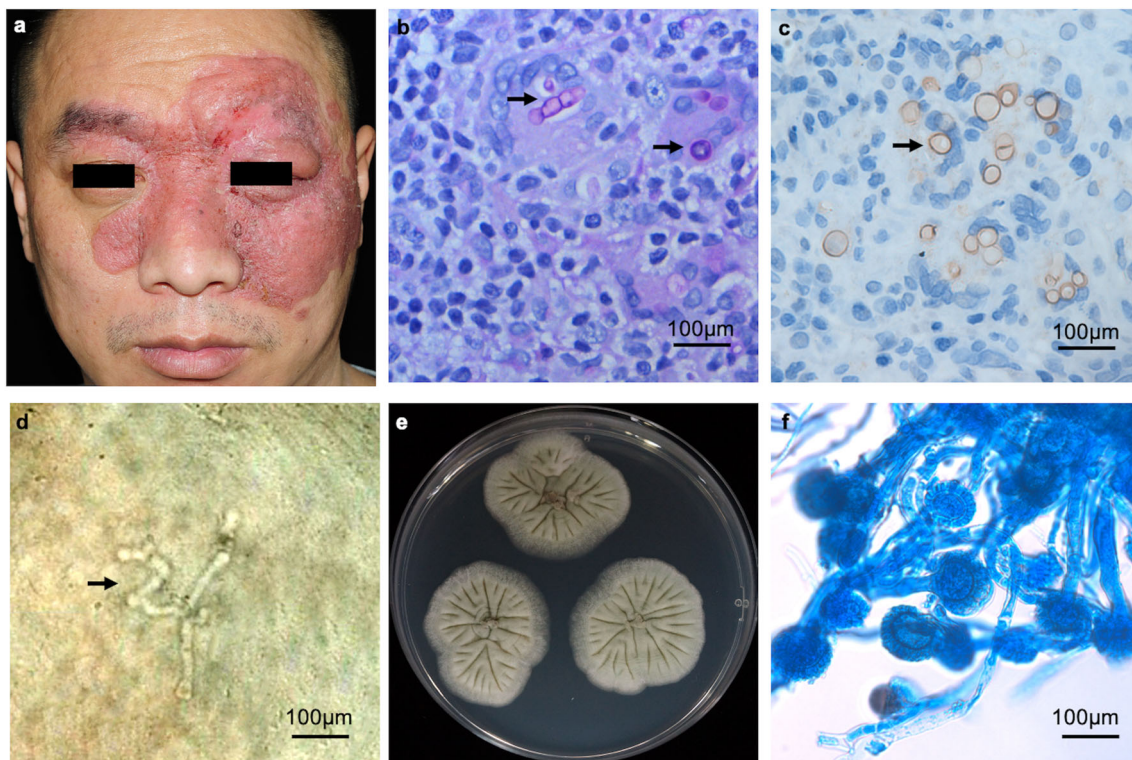
Fig. 1 Clinical features and laboratory findings of the patient. **a** Erythematous plaques with clear border on the patient's face and nose, with slight scale and crust. **b** Histological examination reveals intense inflammatory infiltrations with septate hyphae and conidia noted in multinuclear giant cells (periodic acid–Schiff stain, original magnification × 400). Arrows indicate septate hyphae and conidia. **c** Immunohistochemistry of the tissue sections showing positive *Aspergillus fumigatus* conidia (in brown). Arrow indicates positive *A. fumigatus* conidia. **d** Smear of the lesion showing slender, septate, acute angle branched hyphae with arrow indicated (KOH solution, original magnification × 400). **e** Colonies on potato dextrose agar are dense, light green with a slight creamy-white reverse after 7 days at 28 °C. **f** Microscopic examination of the cultured organisms showing fruiting structures and globular conidiophores (lactophenol cotton blue stain, original magnification × 400). Scale bars in **b**–**d** and **f** = 100 μm

phosphorylation relative to that observed in monocytes from healthy donors (Fig. 3d, e).

## CARD9 Deficiency Compromised Adaptive Immune Responses in Patient-Derived Immune Cells

We assessed the differentiation of T helper (Th) cells in PBMCs from the patient and healthy control participants after stimulation for 6 days. There was significant reduction in the proportions of Th1 (IFN- γ+ CD4+), Th17 (IL-17+CD4+), and Th22 (IL22+IL-17-CD4+) cells in the patient (Fig. 4a–c). We also detected a marked attenuation of IFN-γ, IL-17, and IL-22 expression in the cell culture supernatant (Fig. 4d–f).

Cutaneous Aspergillosis Model in *Card9* KO Mice Could Mimic Clinical Manifestation and Fungal Parasitic Form in the Patient

Considering our clinical and in vitro observations, we used *Card9* KO mice to further study cutaneous aspergillosis by footpad inoculations, as previously described [7]. We included WT and immunosuppressed mice (a neutropenic model) controls to compare their clinical courses, fungal burdens, fungal parasitic forms, and local immune cell infiltration, vis-à-vis *Card9* KO mice. As can be seen in the survival curve and picture of the infection course, WT mice presented mild swelling lesions that nearly resolved spontaneously 4 weeks after the infection (Fig. 5a, c). In contrast, infected *Card9* KO mice were prone to chronic and persistent infections that developed swelling and crust lesions (Fig. 5a, c). As expected, up to 1 week post-infection, all the infected immunosuppressed mice died, because of rapidly growing lesions and dissemination in many organs, probably through blood (Fig. 5a, c). Fungal loads of *A. fumigatus* in the infected footpads were the highest in immunosuppressed and lowest in WT mice on day 3 post-infection (Fig. 5b). Moreover, we did not observe fungal spread in the lungs, kidneys, livers, spleens, and brains in WT and *Card9* KO mice. Histological examination (PAS staining) of infected footpads demonstrated diverse fungal parasitic forms in different groups, with limited conidia in WT mice, germinated conidia with short hyphae in *Card9* KO mice, and aggregate long hyphae in immunosuppressed mice (Fig. 5d). Both the clinical course and the fungal

Fig. 2 Identification and characterization of CARD9 deficiency. **a** Sanger sequencing of *CARD9* showing a homozygous frame-shift mutation in exon 6 (c.819_820insG, p.D274fsX60) in the patient. The patient's son is a heterogeneous carrier of the same mutation. The mutation site is indicated with arrows. **b** Detection of CARD9 protein: electrophoretic analysis of proteins from peripheral blood mononuclear cells (PBMCs) of the patient confirmed the absence of full-length wild-type CARD9 protein
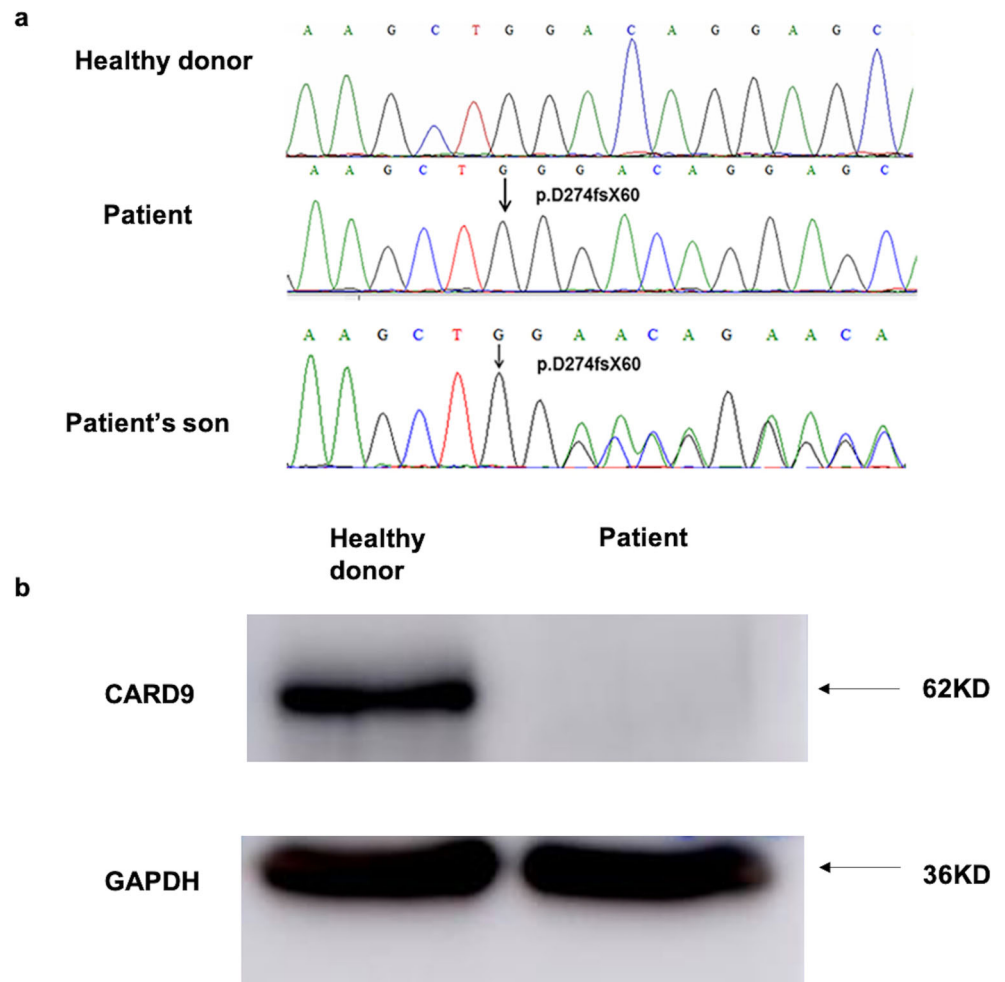
parasitic form in *Card9* KO mice were consistent with those in the patient. Single-cell suspensions derived from the footpad of infected mice showed a significant reduction in neutrophil recruitment at 3 days post-infection in *Card9* KO mice, and there were hardly any neutrophils in immunosuppressed mice locally (Fig. 5e). Similarly, T lymphocyte infiltration was relatively less in *Card9* KO mice at 7 days post-infection (immunosuppressed mice did not survive till day 7) (Fig. 5f). These results were in accordance with the findings in the patient.

Impaired Local Immune Responses in *Card9* KO Mice with Cutaneous Aspergillosis

To study the impairment of specific immune responses against *A. fumigatus* in the skin, we first tested local protein levels of proinflammatory cytokines (IL-1β, TNF-α, and IL-6), and found that *Card9* KO mice and immunosuppressed mice showed significant decline of these cytokines compared to WT mice (Fig. 6a–c). Besides, the levels of cytokines in *Card9* KO mice were slightly higher than those in immunosuppressed mice, with the results being significant for TNF-α

and IL-1β (Fig. 6a–c). We also analyzed the transcription levels of these proinflammatory cytokines and found similar results (data not shown). To verify the mechanism underlying the deficient neutrophil recruitment to the site of infection, we examined the transcription of neutrophils attracting chemokines, and found attenuated CXCL1, CXCL2, and CXCL5 expression in *Card9* KO mice footpad on day 3 post-infection (Fig. 6d–f). We further analyzed local expression of cytokines involved in the adaptive immune response (IFN-γ, IL-17A, and IL-22) on day 7 post-infection (immunosuppressed mice did not survive till day 7), and discovered decreased IFN-γ and IL-22 expression in *Card9* KO mice footpad, although the difference was not significant for the levels of IL-17A (Fig. 6g–i).

Susceptibility of *Card9* KO Mice to Pulmonary Aspergillosis

Interestingly, the patient did not present with pulmonary aspergillosis, even though the lung is the organ that is most frequently affected by *A. fumigatus*. We, therefore, investigated the susceptibility of *Card9* KO mice to pulmonary
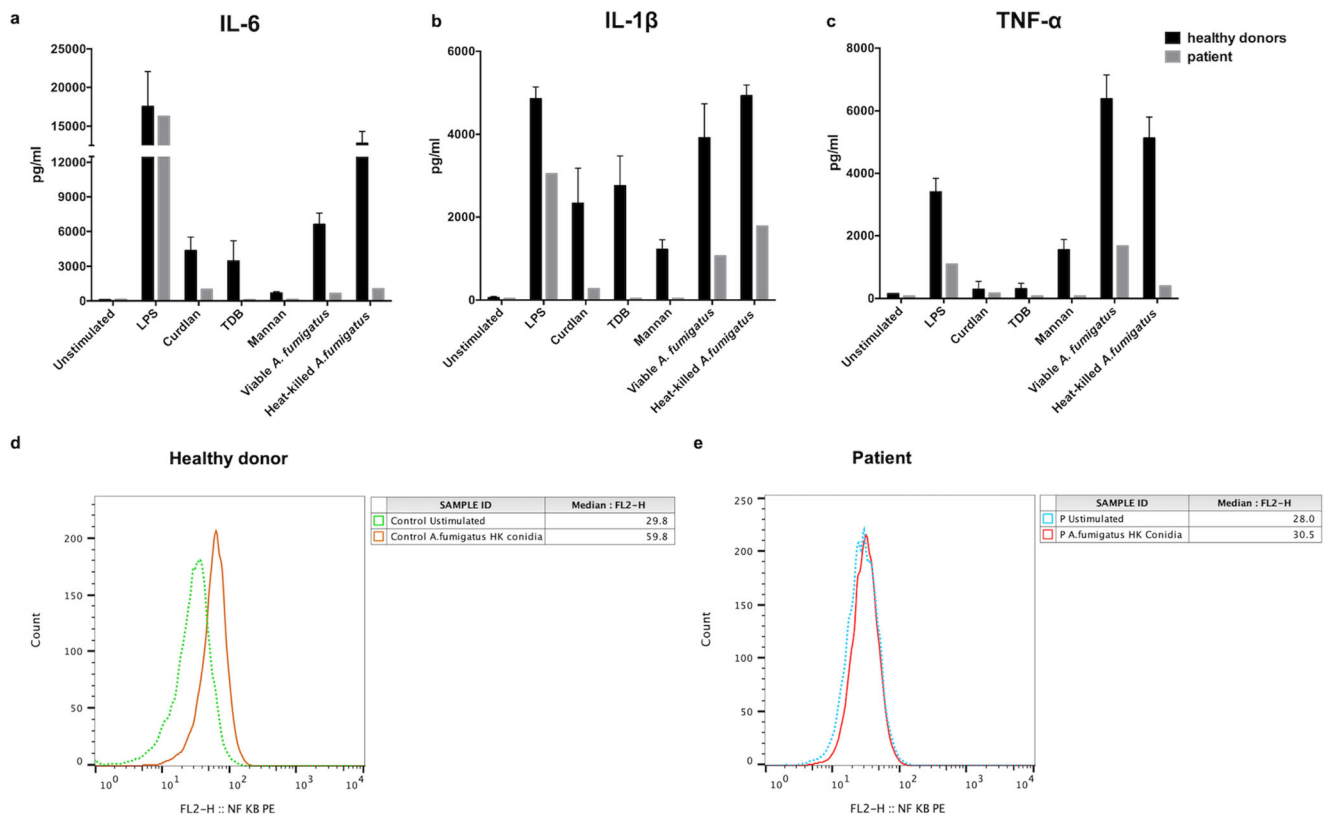
Fig. 3 Detection of innate immune responses in peripheral blood mononuclear cells (PBMCs) derived from the patient and healthy donors ($n = 4$). **a–c** Production of proinflammatory cytokines (IL-6, IL-1β, and TNF-α) in response to 24 h stimulation with lipopolysaccharides (LPS), curdlan, trehalose-6,6-dibehenate (TDB), mannan, and viable and heat-killed (HK) *Aspergillus fumigatus* conidia detected in the supernatants by ELISA. **d–e** NF-κB p65 phosphorylation at Ser536 in peripheral monocytes isolated from the control individuals and the patient, analyzed after stimulation with heat-killed (HK) *A. fumigatus* conidia

aspergillosis. Murine model of pulmonary aspergillosis was created according to the procedures mentioned above. Inhalation of *A. fumigatus* conidia resulted in higher mortality in *Card9* KO mice than in WT mice, but 80% of them survived. In contrast, 100% mortality was noted in immunosuppressed mice at 10 days post-infection (Fig. 7a). Based on general observation, the lung of WT and *Card9* KO mice showed normal appearance on day 3 post-infection, and a mass of hemorrhagic focus was discovered on the surface of the lungs of immunosuppressed mice (indicated by the arrow in Fig. 7b). Comparison of the fungal loads of *A. fumigatus* in the infected lungs revealed that the fungal burden was highest in immunosuppressed mice and lowest in WT mice on day 3 (Fig. 7c). On day 7 post-infection, *A. fumigatus* was cleared up in WT mice and was persistent in *Card9* KO mice. The immunosuppressed group died of extremely high fungal loads and dissemination (fungi were detected in many organs), whereas no fungal dissemination was detected in *Card9* KO mice (data not shown). Histopathology of the lung tissue showed different inflammatory responses in these three groups, with dense inflammatory responses in the WT group, inflammatory response with plenty of eosinophils and few neutrophils in the *Card9* KO group, and mild inflammatory infiltrations in the immunosuppressed group. The fungal parasitic forms in tissue were conidia in the WT group (Fig. 7d) and masses of fungal hyphae in the immunosuppressed group (Fig. 7f). However, quite a few short hyphae and germinated conidia were noted in *Card9* KO mice, which is different from that in the cutaneous aspergillosis model (Fig. 7e).

Discussion

Aspergillus species are saprotrophic fungi that grow on decaying vegetation; they are ubiquitous in nature and spread through spores [8, 9]. *Aspergillus* has emerged as one of the most common causes of death due to infection in severely immunocompromised patients, with mortality rates up to 40% to 50% in patients with acute leukemia and in recipients of hematopoietic stem cell transplantation [10]. *Aspergillus* infection in humans can be divided into several clinical patterns: allergic bronchial pulmonary aspergillosis, chronic pulmonary aspergillosis, aspergilloma, invasive bronchial aspergillosis, invasive pulmonary aspergillosis, and extrapulmonary aspergillosis [10]. Cutaneous aspergillosis is a type of extrapulmonary
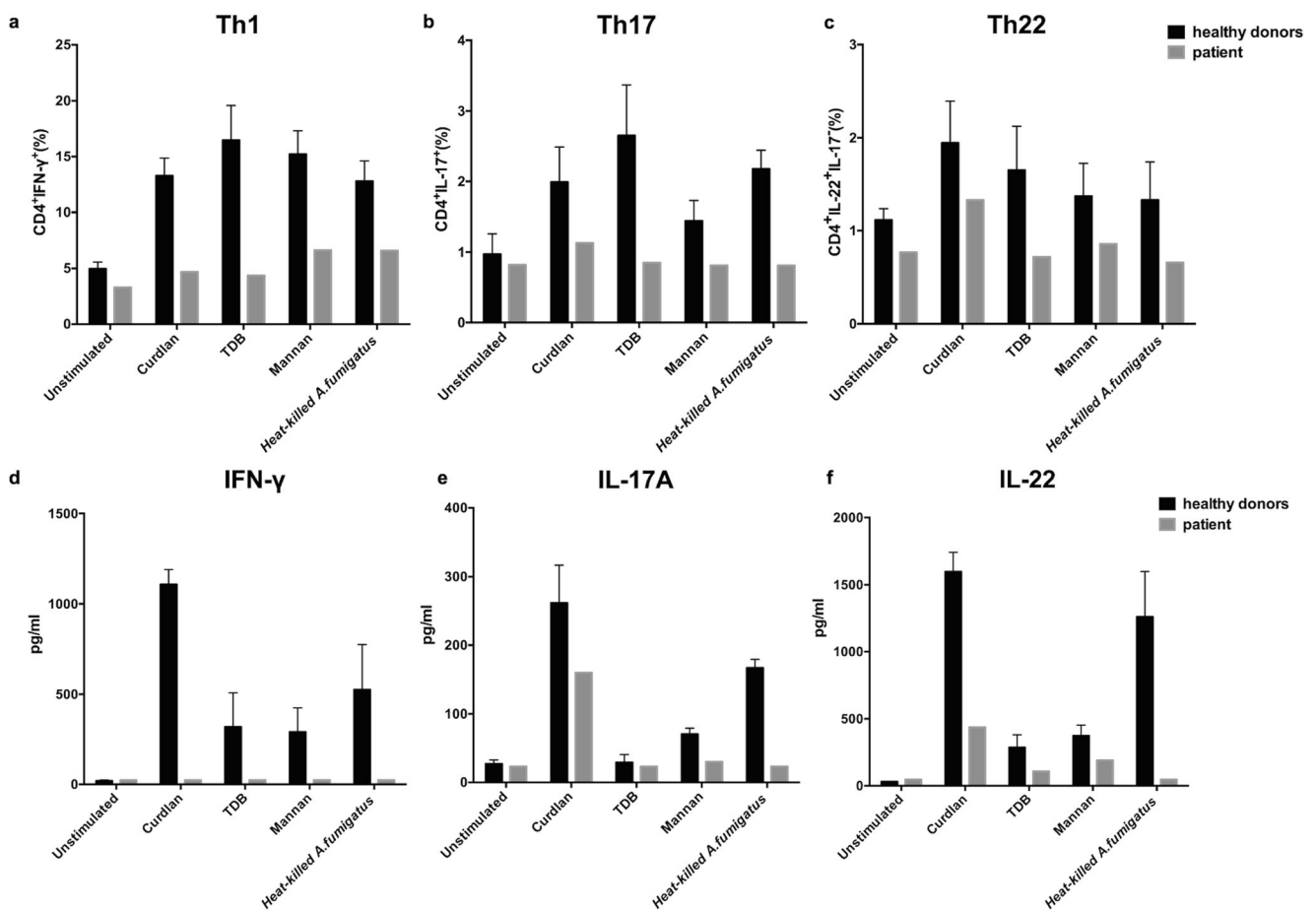
Fig. 4 Detection of adaptive immune responses in peripheral blood mononuclear cells (PBMCs) derived from the patient and healthy donors ($n = 4$). **a–c** Proportions of Th1, Th17, and Th22 cells determined by flow cytometry after 6-day stimulation with curdlan, TDB, mannan, HK *Aspergillus fumigatus* conidia. **d–f** Representative cytokines of Th1, Th17, Th22 cells (IFN- γ, IL-17A, IL-22) measured by ELISA after 6-day stimulation with curdlan, trehalose-6,6-dibehenate (TDB), mannan, and heat-killed (HK) *A. fumigatus* conidia

aspergillosis that may occur either as a primary or secondary infection [11, 12]. PCA is a rare skin infection, mostly caused by *A. flavus*, *A. fumigatus*, *A. terreus*, *A. niger*, and *A. utus* [13]. It is most frequently encountered in immunocompromised patients, with risk factors involving hematologic malignancy, HIV/AIDS, solid organ transplantation, burns, corticosteroid use, diabetes mellitus, chronic granulomatous disease, trauma, and preterm neonates [14]. To date, 41 cases of PCA have been reported in preterm neonates, probably due to the functionally immature immune system and immature skin barrier [15]. However, in the present study, the patient is a worker without any recallable trauma or immunosuppressive therapies. The diagnosis of PCA is difficult because *Aspergillus* spp. is frequently considered a contaminant fungus. Therefore, we conducted direct microscopic examination, tissue culture, and PAS and immunohistochemical staining, and further confirmed the diagnosis of PCA caused by *A. fumigatus*. Immunohistochemistry with specific anti-*Aspergillus* antibodies can identify *Aspergillus* species and differentiate them from other filamentous fungi in situ [16, 17].

To explain the unusual clinical manifestation and the chronic course in this otherwise healthy patient, genetic susceptibility was suspected, and therefore, we performed WES. The previously reported gene, *CARD9*, was screened, and a homozygous frame-shift *CARD9* mutation in exon 6 (c.819_820insG, p.D274fsX60), leading to premature termination codons, was confirmed by Sanger sequencing. To our knowledge, the present case is the first record, in the world, of the pathogenic gene predisposing an individual to PCA. Since its first description in 2009 in a family affected with chronic mucocutaneous candidiasis [18], *CARD9* mutations predisposing humans to fungal infections are being increasingly reported [5]. To date, 24 different deleterious CARD9 alleles have been reported in 65 patients from 14 countries [19], which are linked with various fungal infections including those caused by *Candida* (22 patients) [18, 20–28], dermatophytes (24 patients) [25, 29–35], dematiaceous fungi (14 patients) [6, 36–42], *Aspergillus* (2 patients) [43], *Mucor* (1 patient) [44], *Trichosporon* (1 patient) [45], and *Saprochaete* (1 patient) [46]. Among these, 47 patients were reported to have skin involvement, with pathogens regarding *Candida*,
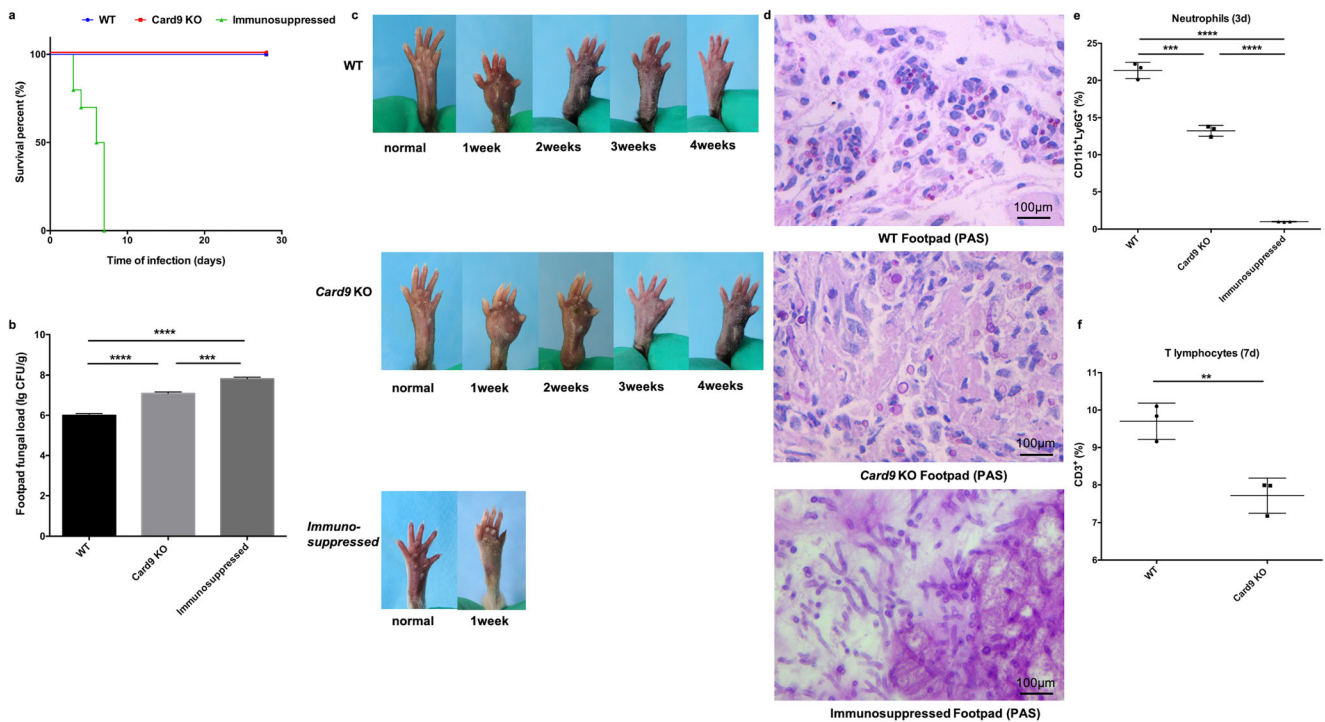
Fig. 5 Cutaneous aspergillosis model in mice. **a** Survival curve in the three groups (WT, *Card9* KO, and immunosuppressed mice) was drawn till day 28 post-infection (2.5 × 10⁹/mL *Aspergillus fumigatus* conidia inoculated subcutaneously; *n* = 10/group). **b** Fungal burden of footpads in *A. fumigatus*–infected WT, *Card9* KO, and immunosuppressed mice on day 3 post-infection (*n* = 3/group). **c** Clinical course of cutaneous *A. fumigatus* infection in WT and *Card9* KO mice. Footpads were injected with 2.5 × 10⁹/mL live *A. fumigatus* conidia and monitored for 4 weeks. **d** Histopathology of footpad biopsies from infected WT, *Card9*

KO, and immunosuppressed mice at 1 week post-infection (PAS staining, original magnification × 400). Scale bars in **d** = 100 μm. **e** Percentage of neutrophils (CD11b+Ly-6G+) in single-cell suspensions derived from the footpad at 3 days post-infection was determined by FACS (*n* = 3/group). **f** Percentage of T lymphocytes (CD3+) in in single-cell suspensions derived from the footpad at 7 days post-infection was determined by FACS (*n* = 3/group). Data are shown as the means ± standard deviation and were analyzed by unpaired *t*-test. **P < 0.01, ***P < 0.001, ****P < 0.0001

dermatophytes, dematiaceous fungi, *Mucor*, and *Trichosporon* [5, 6, 33–35, 39–41, 44, 45]. The face is the most frequently involved site, especially non-dermatophytes, with 14 patients reported so far [6, 36, 38–42, 44, 45]. Moreover, eight unrelated Chinese patients, including the patient in the present study, were reported to hold the same D274fsX60 mutation [6, 36, 38]. These patients share very similar histopathological findings, and their clinical phenotype, fungi involved, treatment, and prognosis of these patients are summarized in Table S2. There is a strong association between the presence of homozygous p.D274fsX60 (c.819-820insG) and disseminated phaeohyphomycosis [19]. Homozygous p.D274fsX60 (c.819-820insG) is one of the three most common mutations in Asia, which has accounted for 17.2% of the Asian cases, whereas homozygous p.Q289X (c.865C > T) accounted for 75% of the African cases [19]. A previous study reported two patients of intra-abdominal aspergillosis with CARD9 deficiency [43]. One patient carrying a homozygous mutation of *CARD9* at the start codon (c.3G > C, p.M1I) died at age 12, with progressive intra-abdominal aspergillosis [43]. The other patient harboring the homozygous Q295X *CARD9* mutation presented with intra-abdominal candidiasis at age 9, and developed central nervous system (CNS)

aspergillosis at age 18 together with intra-abdominal aspergillosis at age 25. It is interesting that neither of the patients developed *Aspergillus* infection in the lung or skin, and our patient did not develop abdominal or CNS aspergillosis. Whether this is due to the specificity of these genotypes, the specific routes of infection, or any other mechanisms, remain unclear [43].

Cytokines released from innate immune cells are crucial for the differentiation of Th cells [47]. Therefore, we used patient PBMCs and observed strong impairment of IL-1β, TNF-α, and IL-6 production in response to stimulation with HK or viable *A. fumigatus* conidia, which are essential for the differentiation, activation, and expansion of Th1, Th17, and Th22 cells [47]. Moreover, our patient exhibited reduced secretion of innate immune cytokines in response to Dectin-1, Mincle, and Dectin-2 agonists, whereas the CARD9-independent response to LPS (a TLR4 agonist) remained unaffected or partially decreased (for unknown reason), which is in agreement with the critical role of CARD9 downstream of these CLRs [4]. In line with our previous studies, proinflammatory cytokine defect probably resulted from the impaired activation of the NF-κB pathway, as suggested by the abnormally low levels of NF-κB p65 phosphorylation observed in monocytes

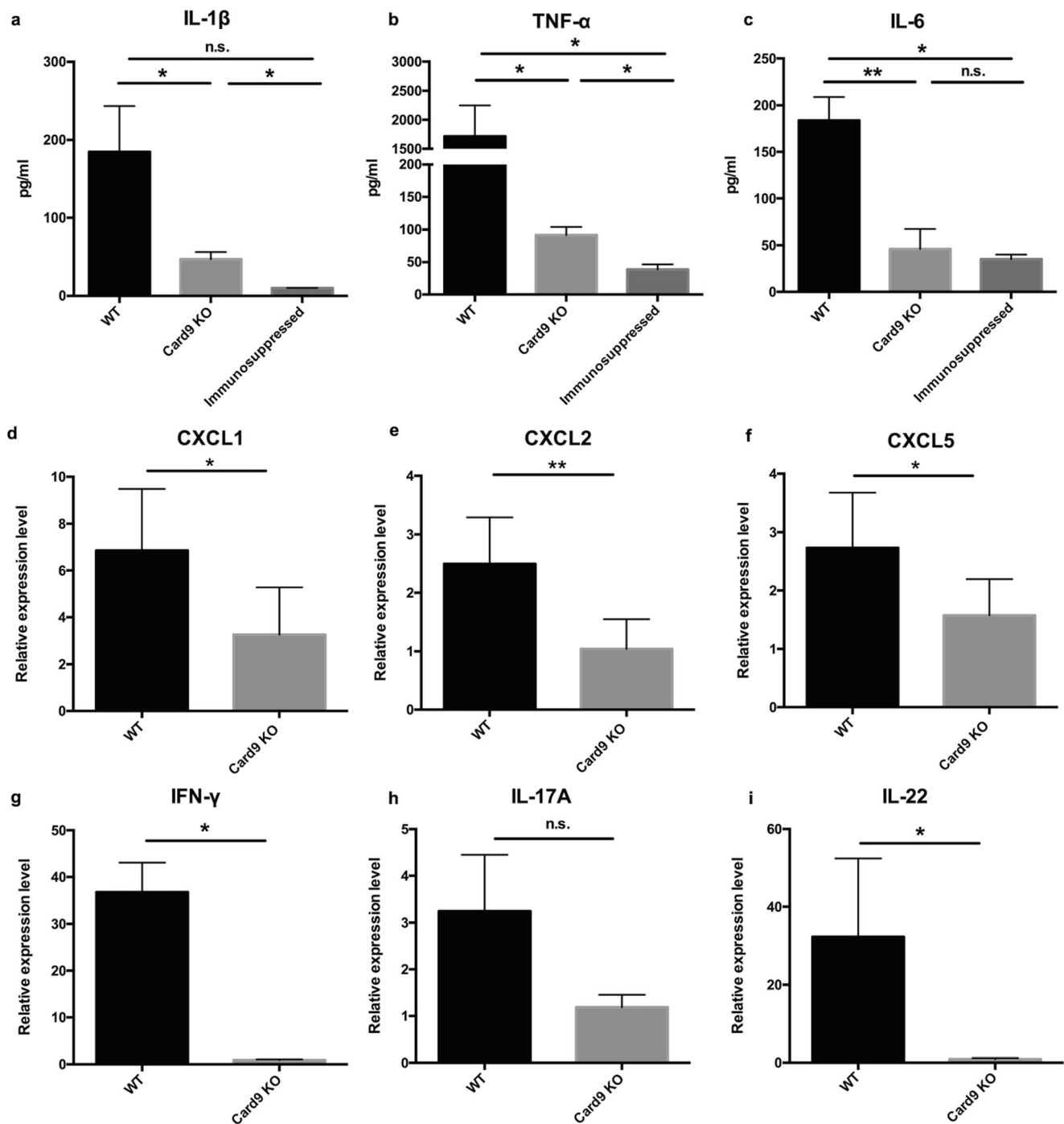**Fig. 6** Detection of local immune responses in murine cutaneous aspergillosis model. **a**–**c** Proinflammatory cytokines (IL-1β, TNF-α, and IL-6) measured in homogenates of footpads from WT, *Card9* KO, and immunosuppressed mice, 3 days post-infection (2.5×10^9/mL *Aspergillus fumigatus* conidia inoculated subcutaneously; $n = 3$/group). **d**–**f** Quantitative real-time reverse transcriptase-PCR analysis of neutrophils attracting chemokines (CXCL1, CXCL2, and CXCL5) in the footpads from WT and *Card9* KO mice, 3 days post-infection (2.5×10^9/mL *A. fumigatus* conidia inoculated subcutaneously; $n = 3$/ group). **g**–**i** Quantitative real-time reverse transcriptase-PCR analysis of adaptive cytokines (IFN-γ, IL-17A, and IL-22) in the footpads from WT and *Card9* KO mice, 7 days post-infection (2.5×10^9/mL *A. fumigatus* conidia inoculated subcutaneously; $n = 3$/group). Data are shown as the means ± standard deviation and were analyzed by unpaired *t*-test. *$P < 0.05$, **$P < 0.01$, n.s. not significant

from patient after stimulation with *A. fumigatus* [38]. It is noteworthy that the percentages of Th1, Th17, and Th22 cells in our patient decreased strikingly when PBMCs were

challenged with HK *A. fumigatus* conidia or relevant polysaccharide, leading to considerable shortage of their effector cytokines, IFN-γ, IL-17A, and IL-22. Th1 and Th17 cells have
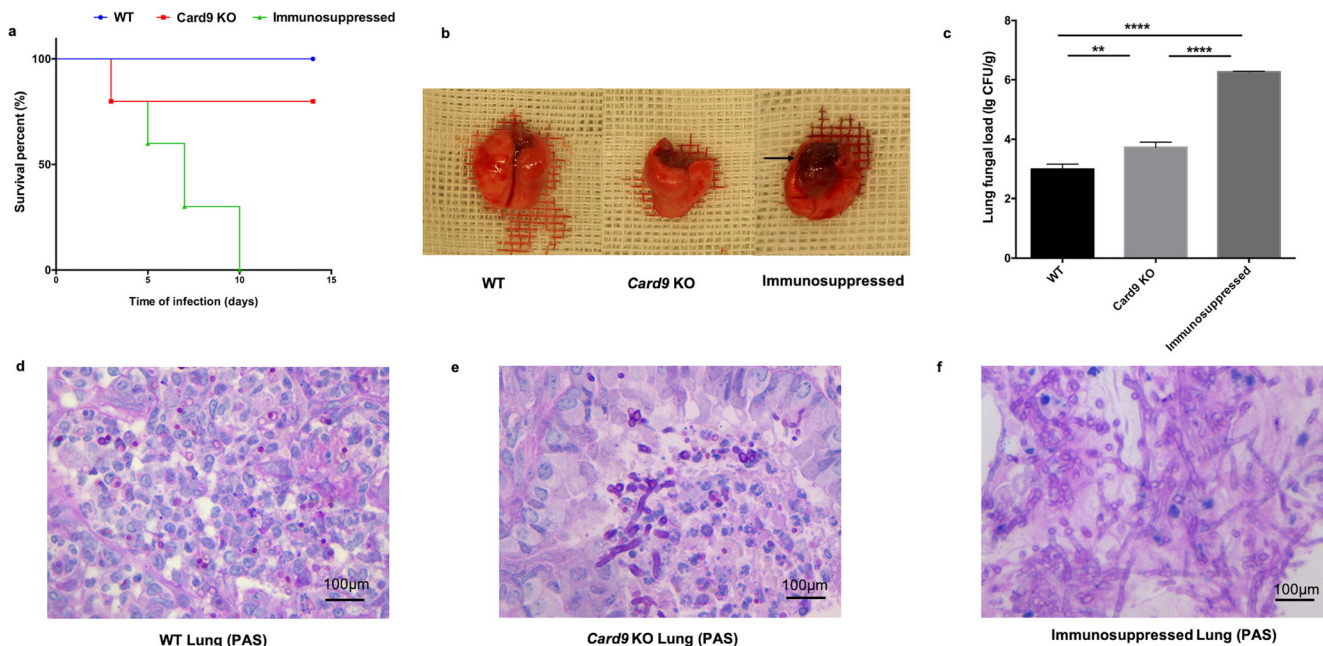
Fig. 7 Pulmonary aspergillosis model in mice. **a** Survival curve in the three groups, WT mice, *Card9* knockout (KO) mice, and immunosuppressed mice, was drawn till day 14 post-infection (2×10^7 *Aspergillus fumigatus* conidia administered intranasally; $n = 10$/group). **b** The general appearance of the infected lung in these three groups on day 3 post-infection. The hemorrhagic focus is indicated by the arrow on the surface of the lung of immunosuppressed mice. **c** Fungal burden of the lung in *A. fumigatus*–infected WT, *Card9* KO, and immunosuppressed mice on day 3 post-infection ($n = 3$/group) (**$**P < 0.01$, ***$*P < 0.0001$). **d**–**f** Histopathology of the lung from the three groups on day 3 post-infection (PAS staining, original magnification × 400). Scale bars in **d**–**f** = 100 μm

been described to have a role in the host response to *A. fumigatus* and contribute to both protective immune responses like fungal clearance and neutrophil recruitment and non-protective (disease-promoting) immune responses [8]. IL-22, which is produced by Th17 cells, Th22 cells, natural-killer cells, or innate lymphoid cells, has been known to exert a protective role against *A. fumigatus* [48].

To further verify our findings in humans, we used *Card9* KO mice to test the cutaneous aspergillosis model. First, we compared the clinical manifestation in the three mice groups. The data suggested that CARD9 deficiency might cause persistent *A. fumigatus* infection in murine footpads compared to that in WT mice; the infection was similar to the chronic granulomatous lesion in the patient. Unlike the persistent infection in *Card9* KO mice, all the infected immunosuppressed mice died in 7 days, which could be explained by the completely suppressed innate and adaptive immune responses, leading to deterioration and dissemination of *A. fumigatus* infection. Second, we compared the histopathology in these groups; unlike the infiltration of various cells in WT mice, *Card9* KO mice lacked adequate infiltration of neutrophils and T lymphocytes. Immunosuppressed mice had an even worse condition, mainly showing necrosis, mycelium clustering, and hardly any infiltration of immune cells, leading to the loss of control on the infection. Neutrophils make up the frontline host defense against fungi. *CARD9* mutations affect both the number of neutrophils recruited and

their killing function. In consistent with previous observations and in the cases of CARD9-deficient patients, we observed significantly decreased neutrophil infiltration in both patient and *Card9* KO mice [20, 38]. T lymphocytes were also impaired in *Card9* KO mice, and this was probably associated with the impaired innate immune responses. Third, we compared the fungal parasitic forms in tissue, and got similar results. The WT and immunosuppressed mice presented with two extreme fungal parasitic forms, with only conidia and only hyphae, respectively. In contrast, *Card9* KO mice showed an intermediate case, with conidia, germinated conidia, and few short hyphae in the tissue, which was similar to the fungal parasitic form in the patient. Lastly, we compared cutaneous immune responses against *A. fumigatus* in these groups at both mRNA and protein levels. At early stages, when innate immunity is playing a dominant role, the production of proinflammatory cytokines and important chemokines recruiting neutrophils was significantly decreased in *Card9* KO mice compared to that in WT mice, but was slightly higher than in immunosuppressed mice, which could explain the persistent *A. fumigatus* infection in *Card9* KO mice and the high mortality in the immunosuppressed group. At later stages, when adaptive immunity is playing a dominant role, there was a marked reduction in the expression levels of IFN-γ and IL-22 mRNAs in *Card9* KO mice (IL-17 was impaired but not significantly), indicating that CARD9 deficiency also impaired the Th1-, Th17-, and Th22-cell

responses against cutaneous *A. fumigatus* infection. However, whether the impaired adaptive immune response is only a side effect of the deficient innate response, or one of the driving factors directly predisposing to fungal infection, still needs further investigations.

The comparison of phenotypes, histopathology, fungal parasitic forms, and local immune responses among the three groups of mice suggested that CARD9 deficiency partially affected the antifungal recognition pathway and the downstream adaptive immune responses in cutaneous *A. fumigatus* infection, which was different from general immunosuppression. Some other pathogen recognition receptors, such as Toll-like receptors (TLRs), which signal independently of CARD9, have also been reported to mediate the recognition of *A. fumigatus* [49]. Therefore, some other compensatory mechanisms might be retained to partially accomplish the antifungal effect in our patient and *Card9* KO mice. We have performed some preliminary studies showing TLR1 might be one of the factors (Fig. S2), which still needs further confirmation. This unique feature of CARD9 deficiency and cutaneous aspergillosis, to some extent, could explain the satisfactory therapeutic effect of oral itraconazole 400 mg/day and good prognosis in this patient.

Taking our previous work into consideration, we showed that *Card9* KO mice were highly susceptible to dematiaceous fungal infections, with mutilation of extremities, dissemination, and presence of numerous hyphae in tissues [7, 38, 50]. *Aspergillus* infection presented better clinical manifestations and lesser hyphae in tissues, probably because the hypoxic cutaneous microenvironments limited the invasive growth of *A. fumigatus*, whereas the slow-growing black fungi could grow well cutaneously. Previous studies have shown that hypoxia at sites of *A. fumigatus* infections influenced the physiology of the pathogen and host immune cells that affected the fungus–host interaction [51]. Moreover, *Aspergillus*, which has different cell wall components compared to dematiaceous fungi, might induce immune response through different pathways.

Aspergillus spp. are known as the most frequent pathogens in the lungs, and CARD9 deficiency is also known to predispose individuals to invasive infections. We, therefore, used a pulmonary aspergillosis model in *Card9* KO mice, and showed their susceptibility to pulmonary aspergillosis, which confirmed the pivotal role of CARD9 in both cutaneous and invasive fungal infections. It may be for the same reasons discussed above that the phenotype of *Card9* KO mice was not as severe as that of immunosuppressed mice. However, if we compare cutaneous and pulmonary aspergillosis in *Card9* KO mice, there were relatively more short hyphae noted in pulmonary aspergillosis. The reason could

be the organ specificity of *A. fumigatus*, which favors fungal growth in the lung (sufficient of oxygen) but not in the skin. Recently, organ-specific functions of CARD9 have been investigated in detail in microglia. The study showed CARD9+ microglia promote antifungal immunity via IL-1β- and CXCL1-mediated neutrophil recruitment, which provided an explanation of CARD9 deficiency causing CNS *Candida* infection [52]. It is interesting that the patient never suffered from pulmonary aspergillosis, which could be because of the control of aspergillosis in the skin, as is observed in *Card9* KO mice; however, the exact mechanism remains to be explored.

In conclusion, we report the case of a patient harboring a *CARD9* mutation who suffered from primary cutaneous aspergillosis. This is, to our knowledge, the first report that links cutaneous aspergillosis to *CARD9* mutation. The patient showed selectively compromised innate and adaptive antifungal responses and increased susceptibility to *A. fumigatus* infection. Interestingly, *Card9* KO mice were susceptible to both cutaneous and pulmonary aspergillosis, but the condition was less severe than in immunosuppressed mice, suggesting that alternative pathways might locally compensate the CARD9 deficiency. This work improves our understanding of the genetic underpinnings of PCA and broadens the phenotypic spectrum of diseases associated with CARD9 deficiency.

Compliance with Ethical Standards

This study was approved by the Clinical Research Ethics Committee of the Peking University First Hospital. We obtained blood samples from the patient, his son, and three ethnically matched healthy volunteers, after obtaining informed consent. The patient gave permission to publish his images and medical information. Animal studies were approved by the Institutional Ethics Committee of Peking University First Hospital in accordance with the institutional guidelines.

Conflict of Interest   The authors declare that they have no conflicts of interest.

References

1. Tatara AM, Mikos AG, Kontoyiannis DP. Factors affecting patient outcome in primary cutaneous aspergillosis. Medicine (Baltimore). 2016;95(26):e3747.

2. Darr-Foit S, Schliemann S, Scholl S, Hipler UC, Elsner P. Primary cutaneous aspergillosis - an uncommon opportunistic infection review of the literature and case presentation. J Dtsch Dermatol Ges. 2017;15(8):839–41.

3. Liu X, Yang J, Ma W. Primary cutaneous aspergillosis caused by Aspergillus fumigatus in an immunocompetent patient. Medicine (Baltimore). 2017;96(48):e8916.

4. Zhong X, Chen B, Yang L, Yang Z. Molecular and physiological roles of the adaptor protein CARD9 in immunity. Cell Death Dis. 2018;9(2):52.

5. Corvilain E, Casanova J-L, Puel A. Inherited CARD9 deficiency: invasive disease caused by ascomycete fungi in previously healthy children and adults. J Clin Immunol. 2018;38(6):656–93.

6. Huang C, Zhang Y, Song Y, Wan Z, Wang X, Li R. Phaeohyphomycosis caused by Phialophora americana with CARD9 mutation and 20-year literature review in China. Mycoses. 2019;62(10):908–19.

7. Wu W, Zhang R, Wang X, Song Y, Liu Z, Han W, et al. Impairment of immune response against dematiaceous fungi in Card9 knockout mice. Mycopathologia. 2016;181(9–10):631–42.

8. van de Veerdonk FL, Gresnigt MS, Romani L, Netea MG, Latgé JP. Aspergillus fumigatus morphology and dynamic host interactions. Nat Rev Microbiol. 2017;15(11):661–74.

9. Kartik M, Kanala A, Sunilnadikuda, Rao SM, Prakasham PS. Invasive mediastinal Aspergillosis in immunocompetent male with invasion of left atrium and hilar structures. Indian J Crit Care Med. 2017;21(6):408–11.

10. Latgé JP, Chamilos G. Aspergillus fumigatus and Aspergillosis in 2019. Clin Microbiol Rev. 2019;33(1):e00140–18.

11. Venugopal TV, Venugopal PV. Primary cutaneous aspergillosis from Tamilnadu diagnosed by fine needle aspiration cytology. Med Mycol Case Rep. 2012;1(1):103–6.

12. Bernardeschi C, Foulet F, Ingen-Housz-Oro S, Ortonne N, Sitbon K, Quereux G, et al. Cutaneous invasive aspergillosis: retrospective multicenter study of the French invasive-aspergillosis registry and literature review. Medicine (Baltimore). 2015;94(26):e1018.

13. Fernandez-Flores A, Saeb-Lima M, Arenas-Guzman R. Morphological findings of deep cutaneous fungal infections. Am J Dermatopathol. 2014;36(7):531–53 quiz 554–6.

14. Shields BE, Rosenbach M, Brown-Joel Z, Berger AP, Ford BA, Wanat KA. Angioinvasive fungal infections impacting the skin: background, epidemiology, and clinical presentation. J Am Acad Dermatol. 2019;80(4):869–80.e5.

15. Gallais F, Denis J, Koobar O, Dillenseger L, Astruc D, Herbrecht R, et al. Simultaneous primary invasive cutaneous aspergillosis in two preterm twins: case report and review of the literature. BMC Infect Dis. 2017;17(1):535.

16. Challa S, Uppin SG, Uppin MS, Pamidimukkala U, Vemu L. Diagnosis of filamentous fungi on tissue sections by immunohistochemistry using anti-aspergillus antibody. Med Mycol. 2015;53(5):470–6.

17. Jung J, Park YS, Sung H, Song JS, Lee S-O, Choi S-H, et al. Using of immunohistochemistry to assess the accuracy of histomorphologic diagnosis of aspergillosis and mucormycosis. Clin Infect Dis. 2015;61(11):1664–70.

18. Glocker EO, Hennigs A, Nabavi M, Schäffer AA, Woellner C, Salzer U, et al. A homozygous CARD9 mutation in a family with susceptibility to fungal infections. N Engl J Med. 2009;361(18):1727–35.

19. Vaezi A, Fakhim H, Abtahian Z, Khodavaisy S, Geramishoar M, Alizadeh A, et al. Frequency and geographic distribution of CARD9 mutations in patients with severe fungal infections. Front Microbiol. 2018;9:2434.

20. Drewniak A, Gazendam RP, Tool AT, van Houdt M, Jansen MH, van Hamme JL, et al. Invasive fungal infection and impaired neutrophil killing in human CARD9 deficiency. Blood. 2013;121(13):2385–92.

21. Gavino C, Cotter A, Lichtenstein D, Lejtenyi D, Fortin C, Legault C, et al. CARD9 deficiency and spontaneous central nervous system candidiasis: complete clinical remission with GM-CSF therapy. Clin Infect Dis. 2014;59(1):81–4.

22. Drummond RA, Collar AL, Swamydas M, Rodriguez CA, Lim JK, Mendez LM, et al. CARD9-dependent neutrophil recruitment protects against fungal invasion of the central nervous system. PLoS Pathog. 2015;11(12):e1005293.

23. Herbst M, Gazendam R, Reimnitz D, Sawalle-Belohradsky J, Groll A, Schlegel PG, et al. Chronic Candida albicans meningitis in a 4-year-old girl with a homozygous mutation in the CARD9 gene (Q295X). Pediatr Infect Dis J. 2015;34(9):999–1002.

24. Lanternier F, Mahdaviani SA, Barbati E, Chaussade H, Koumar Y, Levy R, et al. Inherited CARD9 deficiency in otherwise healthy children and adults with Candida species-induced meningoencephalitis, colitis, or both. J Allergy Clin Immunol. 2015;135(6):1558–68.e2.

25. Alves de Medeiros AK, Lodewick E, Bogaert DJ, Haerynck F, Van Daele S, Lambrecht B, et al. Chronic and invasive fungal infections in a family with CARD9 deficiency. J Clin Immunol. 2016;36(3):204–9.

26. Celmeli F, Oztoprak N, Turkkahraman D, Seyman D, Mutlu E, Frede N, et al. Successful granulocyte colony-stimulating factor treatment of relapsing Candida albicans meningoencephalitis caused by CARD9 deficiency. Pediatr Infect Dis J. 2016;35(4):428–31.

27. Gavino C, Hamel N, Zeng JB, Legault C, Guiot MC, Chankowsky J, et al. Impaired RASGRF1/ERK-mediated GM-CSF response characterizes CARD9 deficiency in French-Canadians. J Allergy Clin Immunol. 2016;137(4):1178–88.e7.

28. Jones N, Garcez T, Newman W, Denning D. Endogenous Candida endophthalmitis and osteomyelitis associated with CARD9 deficiency. BMJ Case Rep. 2016;2016:bcr2015214117.

29. Lanternier F, Pathan S, Vincent QB, Liu L, Cypowyj S, Prando C, et al. Deep dermatophytosis and inherited CARD9 deficiency. N Engl J Med. 2013;369(18):1704–14.

30. Grumach AS, de Queiroz-Telles F, Migaud M, Lanternier F, Filho NR, Palma SM, et al. A homozygous CARD9 mutation in a Brazilian patient with deep dermatophytosis. J Clin Immunol. 2015;35(5):486–90.

31. Jachiet M, Lanternier F, Rybojad M, Bagot M, Ibrahim L, Casanova JL, et al. Posaconazole treatment of extensive skin and nail dermatophytosis due to autosomal recessive deficiency of CARD9. JAMA Dermatol. 2015;151(2):192–4.

32. Boudghene Stambouli O, Amrani N, Boudghene Stambouli K, Bouali F. Dermatophytic disease with deficit in CARD9: a new case with a brain impairment. J Mycol Med. 2017;27(2):250–3.

33. Zhang Y, Mijiti J, Huang C, Song Y, Wan Z, Li R, et al. Deep dermatophytosis caused by Microsporum ferrugineum in a patient with CARD9 mutations. Br J Dermatol. 2019;181(5):1093–5.

34. Nazarian RM, Lilly E, Gavino C, Hamilos DL, Felsenstein D, Vinh DC, et al. Novel CARD9 mutation in a patient with chronic invasive dermatophyte infection (tinea profunda). J Cutan Pathol. 2020;47(2):166–70.

35. Huang C, Peng Y, Zhang Y, Li R, Wan Z, Wang X. Deep dermatophytosis caused by Trichophyton rubrum. Lancet Infect Dis. 2019;19(12):1380.

36. Wang X, Wang W, Lin Z, Wang X, Li T, Yu J, et al. CARD9 mutations linked to subcutaneous phaeohyphomycosis and TH17 cell deficiencies. J Allergy Clin Immunol. 2014;133(3):905–8.e3.

37. Lanternier F, Barbati E, Meinzer U, Liu L, Pedergnana V, Migaud M, et al. Inherited CARD9 deficiency in 2 unrelated patients with invasive Exophiala infection. J Infect Dis. 2015;211(8):1241–50.

38. Wang X, Zhang R, Wu W, Song Y, Wan Z, Han W, et al. Impaired specific antifungal immunity in CARD9-deficient patients with phaeohyphomycosis. J Invest Dermatol. 2018;138(3):607–17.

39. Arango-Franco CA, Moncada-Velez M, Beltran CP, Berrio I, Mogollon C, Restrepo A, et al. Early-onset invasive infection due to Corynespora cassiicola associated with compound heterozygous CARD9 mutations in a Colombian patient. J Clin Immunol. 2018;38(7):794–803.

40. Guo Y, Zhu Z, Gao J, Zhang C, Zhang X, Dang E, et al. The phytopathogenic fungus Pallidocercospora crystallina-caused localized subcutaneous phaeohyphomycosis in a patient with a homozygous missense CARD9 mutation. J Clin Immunol. 2019;39(7):713–25.

41. Wang C, Xing H, Jiang X, Zeng J, Liu Z, Chen J, et al. Cerebral phaeohyphomycosis caused by Exophiala dermatitidis in a Chinese CARD9-deficient patient: a case report and literature review. Front Neurol. 2019;10:938.

42. Perez L, Messina F, Negroni R, Arechavala A, Bustamante J, Oleastro M, et al. Inherited CARD9 deficiency in a patient with both Exophiala spinifera and Aspergillus nomius severe infections. J Clin Immunol. 2020;40(2):359–66.

43. Rieber N, Gazendam RP, Freeman AF, Hsu AP, Collar AL, Sugui JA, et al. Extrapulmonary Aspergillus infection in patients with CARD9 deficiency. JCI Insight. 2016;1(17):e89890.

44. Wang X, Wang A, Wang X, Li R, Yu J. Cutaneous mucormycosis caused by Mucor irregularis in a patient with CARD9 deficiency. Br J Dermatol. 2019;180(1):213–4.

45. Quan C, Li X, Shi RF, Zhao XQ, Xu H, Wang B, et al. Recurrent fungal infections in a Chinese patient with CARD9 deficiency and a review of 48 cases. Br J Dermatol. 2018;180(5):1221–5.

46. Erman B, Firtina S, Aksoy BA, Aydogdu S, Genc GE, Dogan O, et al. Invasive Saprochaete capitata infection in a patient with autosomal recessive CARD9 deficiency and a review of the literature. J Clin Immunol. 2020;40(3):466–74.

47. Lionakis MS, Iliev ID, Hohl TM. Immunity against fungi. JCI Insight. 2017;2(11):e93156.

48. Gessner MA, Werner JL, Lilly LM, Nelson MP, Metz AE, Dunaway CW, et al. Dectin-1-dependent interleukin-22 contributes to early innate lung defense against Aspergillus fumigatus. Infect Immun. 2012;80(1):410–7.

49. Rubino I, Coste A, Le Roy D, Roger T, Jaton K, Boeckh M, et al. Species-specific recognition of Aspergillus fumigatus by Toll-like receptor 1 and Toll-like receptor 6. J Infect Dis. 2012;205(6):944–54.

50. Wu W, Zhang R, Wang X, Song Y, Li R. Subcutaneous infection with dematiaceous fungi in Card9 knockout mice reveals association of impair neutrophils and Th cell response. J Dermatol Sci. 2018;92(2):215–8.

51. Grahl N, Shepardson KM, Chung D, Cramer RA. Hypoxia and fungal pathogenesis: to air or not to air? Eukaryot Cell. 2012;11(5):560–70.

52. Drummond RA, Swamydas M, Oikonomou V, Zhai B, Dambuza IM, Schaefer BC, et al. CARD9$^+$ microglia promote antifungal immunity via IL-1β- and CXCL1-mediated neutrophil recruitment. Nat Immunol. 2019;20(5):559–70.